Journal of Engineering and Technology for Industrial Applications

ITEGAM-JETIA

Manaus, v.12 n.58, p. 53-63. March/April, 2026.
DOI: https://doi.org/10.5935/jetia.v12i58.2763

ISSN ONLINE: 2447-0228

RESEARCH ARTICLE OPEN ACCESS

ELECTROCHEMICAL POTENTIAL AND CHARACTERIZATION OF $NIFE_2O_4$/CU-1 AND $NIFE_2O_4$/CU-2

Naveen Chandra Joshi[1]*, Khundrakpam Somen Singh[2], B. S. Rawat[3]

[1]Department of Chemistry, Uttaranchal University Dehradun, 248007 (India).
[2]Department of Chemistry, Graphic Era (Deemed to be University) Dehradun, 248002 (India).
[3]Department of Physics, Uttaranchal University Dehradun, 248007 (India).

[1]https://orcid.org/0000-0003-0095-9695, [2] https://orcid.org/0009-0006-4922-6133, [3]https://orcid.org/0000-0001-6926-5259

Email: somenkhundrakpam12@gmail.com, *drnaveen06joshi@gmail.com, park_bhupendra@hotmail.com

ARTICLE INFO

Article History
Received: November 30, 2025
Reviewed: December 10, 2025
Accepted: December 15, 2025
Published: March 31, 2026

Keywords:
Supercapacitors;
$NiFe_2O_4$/Cu-1 and $NiFe_2O_4$/Cu-2;
Synthesis; Characterization;
Electrochemical study.

ABSTRACT

Ferrite-based materials have been studied for the electrode materials for supercapacitors because of their low cost and rapid, reversible surface Faradaic reactions. In this study, we have developed two electrode materials named $NiFe_2O_4$/Cu-1 and $NiFe_2O_4$/Cu-2. The fabrication method was found to be inexpensive, effective, and efficient. The synthesized materials were analyzed via FTIR, XRD, SEM, and TEM methods. FTIR results indicated the presence of O-H, C-H, C-O, Ni-Fe, Fe-Cu, Cu-O, etc. bonds on the surface of these materials. The XRD patterns indicated the amorphous nature of $NiFe_2O_4$ and the semi-crystalline nature of $NiFe_2O_4$/Cu-1 and $NiFe_2O_4$/Cu-2. The SEM analysis indicated that the particles are semi-spherical, and some are irregular in $NiFe_2O_4$. The sphere-shaped particles were observed in the case of $NiFe_2O_4$/Cu-1 and $NiFe_2O_4$/Cu-2, respectively. The electrochemical study has been conducted using different electrochemical parameters. The $NiFe_2O_4$/Cu-2 exhibited a power density of 4992 W/kg, an energy density of 5.9 Wh/kg, a retention of 91.3%, and a specific capacitance of 222 F/g. It was additionally found that the $NiFe_2O_4$/Cu-2 was appropriate for device systems with a 42 F/g specific capacitance (under a 2-electrode system).

I. INTRODUCTION

Green energy sources offer affordable, renewable energy alongside lowering greenhouse gas emissions and promoting economic growth. Energy storage technology is a sustainable way to achieve the goal of a net-zero carbon footprint and a green energy transition. This technology promotes the reduction of the emission of greenhouse gases. Energy storage mitigates the fundamental fluctuation of renewable energy, manages high demand periods, and allows the integration of small-scale systems[1]. To maintain system frequency and voltage, smooth power, and provide fault ride-through assistance, energy storage has been considered to be a revolutionary solution for the integration of variable renewables [2]. One of the main solutions to the energy challenges facing our civilization is electrical energy storage. The most common rechargeable electrochemical energy storage systems include metal-air batteries, lithium-ion batteries, supercapacitors, and sodium-ion batteries, which are utilized in different electronic gadgets and transportation[3].

Supercapacitors offer many advantages, such as long life, efficient charge and discharge, high power density, flexibility, and lightweightness. Studies are going on for the development of efficient and low-cost electrode materials. The green energy goals need environmentally friendly, durable, and electrochemically efficient electrode materials[4], [5]. The choice of electrolytes for supercapacitors also affects the electrochemical parameters. The choice of electrolyte depends on the application and performance requirements. The aqueous electrolytes, such as KOH, have high ionic conductivity, decrease the internal resistance, are low-cost, and are suitable for large-scale systems. This type of electrolyte promotes rapid charge-discharge cycles and power density[6], [7]. Electrode materials for supercapacitors must have high electrical conductivity, excellent electrochemical stability, and large surface area and porosity. Some common electrode materials include carbon-based, metal- and metal-oxide-based, conducting polymers, and hybrid materials of all of these[8].

The term "ferrite," which comes from the Latin word "ferrum," refers to ceramic compositions where iron oxide is combined with other metals. Since ferrites are ferrimagnetic, a magnetic field may readily attract them[9]. These materials have been used in solar energy devices, batteries, supercapacitors, biomedicals, electronic devices, and magnetic fluids [10], [11]. Low magnetic loss, high magnetic permeability, and moderate coercivity are some of the outstanding magnetic properties of $NiFe_2O_4$ that have generated attention for applications in electronics, sensors, energy storage systems, and telecommunications [12]. In nickel ferrite (NiFe2O4), nickel and iron cations partially occupy a face-centered cubic lattice of oxygen atoms with interpenetrating tetrahedral and octahedral sites. This separation allows adjustable magnetic characteristics. Doping with foreign metals affects the magnetism of the material via altering cation occupancy and interactions[13]. The materials based on $NiFe_2O_4$ shows high electrochemical stability and efficiency and are found suitable for supercapacitors[14]. Cu-based materials have also been recognized for their low cost, efficiency, and outstanding electrochemical performances. They can effectively be utilized in the development of hybrid electrode materials for supercapacitors[15]. The characteristics such as non-toxicity, easy preparation, and outstanding optical, electrochemical, and electric properties make them potential candidates for the supercapacitors[4]. Copper (Cu) significantly improves the electrochemical performance of supercapacitors. The remarkable redox potential, high electrical conductivity, and unique structural features of Cu enhance the supercapacitive performance of electrodes. Cu-based materials are capable of enhancing charge transfer and redox behavior and lowering electrical resistance. These materials are also able to boost cyclic stability and specific capacitance[15], [16].

Similar work has been done by other researchers in the recent past. The electrochemical potential of a nanocomposite based on Ni/$CoFe_2O_4$/MXene for supercapacitors was reported by Infancy et al.[17]. A 1 M KOH solution was used for the electrochemical investigation. Ni/$CoFe_2O_4$ and Ni/$CoFe_2O_4$/MXene samples showed specific capacitances of 361 C/g and 367 C/g, respectively. The supercapacitive performance of a nanocomposite based on cobalt ferrite ($CoFe_2O_4$) and polyaniline (PANI) was investigated by Mandal and Dasmahapatra[18]. With a good cyclic life (~91% retention after the 1500 cycles), the supercapacitor electrode demonstrated a maximum specific capacitance of 460.1 F/g at 0.5 A/g. The electrochemical potential of $MnFe_2O_4$ using multiple electrolytes, including 1 M $LiNO_3$, 1 M Li_3PO_4, and KOH, was reported by Vignesh et al.[19]. Maximum specific capacitances of 173, 31, and 430 F/g were achieved in a three-electrode setup, which corresponded to electrolytes of 3.5 M KOH, 1 M $LiNO_3$, and 1 M Li_3PO_4, respectively. Also, at the high current density of 1.5 A/g, the specific capacitance of 105% was maintained after 10,000 cycles, and the coulombic efficiency of all 10,000 cycles stayed constant, indicating the exceptional electrochemical durability of $MnFe_2O_4$. $MnFe_2O_4$/rGO nanocomposite for supercapacitors was reported by Shih and Tseng[20]. A high specific capacitance of 196.6 F/g at 0.5 A/g was evaluated, and 90.22% of the capacitance was retained after 6000 cycles. The synergistic effects of rGO and $MnFe_2O_4$ contributed to the improved performance. In the present work, we have improved the electrochemical performances of $NiFe_2O_4$ after incorporating it with Cu. The achieved outstanding electrochemical ability of Cu-blended $NiFe_2O_4$ makes them promising candidates for electrode material of supercapacitors.

II. MATERIALS AND METHOD

All chemicals used were of AR grade. These chemicals were purchased from Merck, SRL, and LOBA. In this work, potassium hydroxide (KOH), sodium hydroxide (NaOH), lithium nitrate (LiNO3), lithium phosphate (Li3PO4), copper acetate [Cu(CH3COO)2], nickel nitrate [Ni(NO3)2], ferric nitrate [Fe(NO3)3], polyvinylidene fluoride (PVDF), N-methyl-2-pyrrolidone (NMP), and acetone (CH3COCH3) were used.

II.1 SYNTHESIS OF $NIFE_2O_4$, $NIFE_2O_4$/CU-1, AND $NIFE_2O_4$/CU-2

Dissolve Ni(NO3)2 and Fe(NO3)3 in distilled water in a ratio of 1:2 and shake the mixture for 35 min. Add 0.5 g of citric acid to this mixture and allow it to shake for 35 min. Then a few drops of 0.1 M NaOH were added, and the mixture was stirred for 1 h. After centrifugation, the $NiFe_2O_4$ was collected and dried in a hot air oven. The obtained $NiFe_2O_4$ was calcined at 650°C for 3.5 h. Now 100 and 200 mg of Cu was added to 1 g of $NiFe_2O_4$ using $Cu(CH_3COO)_2$. These amounts have been calculated stoichiometrically. The obtained mixtures were crushed for 1 h and then sonicated with distilled water for 2h. The obtained mixtures have also been calcined at 6500C for 3.5 h. Finally, $NiFe_2O_4$/Cu-1 (100 mg Cu) and $NiFe_2O_4$/Cu-2 (200 mg Cu) were obtained for characterization and electrochemical studies. The overall synthetic method is presented in Figure 1.

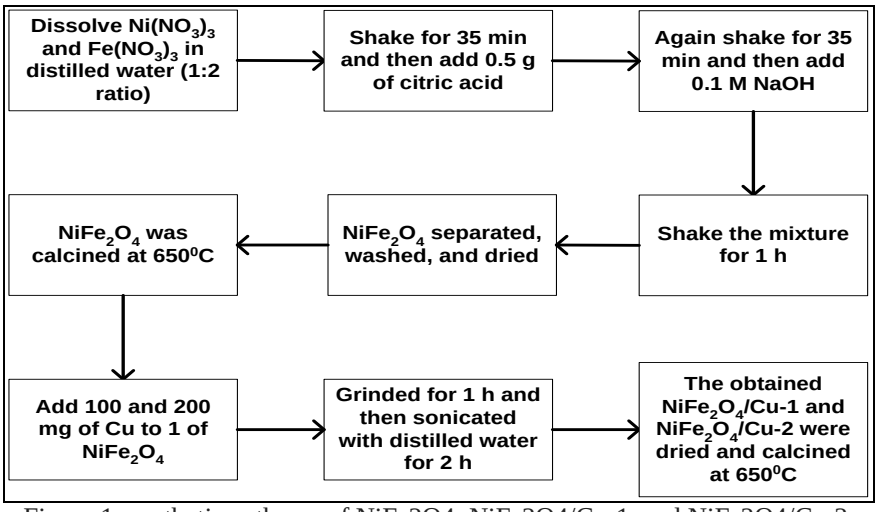

Figure 1: synthetic pathway of NiFe2O4, NiFe2O4/Cu-1, and NiFe2O4/Cu-2.
Source: Authors, (2026).

II.2 CHARACTERIZATION OF $NIFE_2O_4$, $NIFE_2O_4$/CU-1, AND $NIFE_2O_4$/CU-2

The characterization of $NiFe_2O_4$/Cu-1 and $NiFe_2O_4$/Cu-2 was done using FTIR (Fourier transform infrared spectroscopy; Model: Thermo Scientific Nicolet Summit Lite), XRD (X-ray diffraction; Model: Rigaku), SEM (Scanning electron microscopy; Model: Carl Zeiss EV018), and TEM (Transmission electron microscopy; Model: Talos L120C) techniques. The basic description these methods is given as below:

FTIR

FTIR is an advanced and high-precision instrument and is generally used to detect the presence of different chemical bonds or functional groups on the surfaces of molecules or nanomaterials. It enables the identification of molecules with different infrared spectra by focusing on atomic vibrations[21].

XRD

XRD is widely used for the characterization of nanomaterials. The characteristics of the material, such as strain, crystallite size, and crystal structure, are easily determined. The crystalline structure of a material is determined by utilizing Bragg's law and a detector to examine interference caused by atoms scattering X-rays[22].

SEM

SEM is used to provide morphology of nanomaterials. This technique uses an electron beam with an acceleration of up to 30 kV to study the surface of a material. In order to create an image, detectors collect the signals that the specimen emits. Information about composition and topography is provided by backscattered electrons[23].

TEM

TEM allows for imaging at the nanoscale and sub-nanometer scale by interacting with ultra-thin specimen layers on a copper grid using a high-energy electron beam[24].

II.3 ELECTROCHEMICAL STUDY

The electrode slurries of $NiFe_2O_4$/Cu-1 and $NiFe_2O_4$/Cu-2 were prepared by mixing 80 mg of $NiFe_2O_4$/Cu-1 or $NiFe_2O_4$/Cu-2, 10 mg of PVDF, and 10 mg of carbon black in NMP. These slurries were coated over Ni-foam and then allowed to dry for 6 h at 80°C. The electrochemical study of $NiFe_2O_4$/Cu-1 and $NiFe_2O_4$/Cu-2 was conducted using Ag/AgCl, Pt, and working electrodes in 1M KOH solution. The different electrochemical parameters, such as cyclic voltammetry (CV), capacity retention, GCD (Galvanostatic charge-discharge) , and EIS (Electrochemical impedance spectroscopy), have been used. The specific capacitance of $NiFe_2O_4$/Cu-1 and $NiFe_2O_4$/Cu-2 was evaluated using the following equation:

$$C = I\Delta t/m\Delta V \quad (1)$$

In this equation, I, m, ΔV and Δt are current, mass of active materials, voltage difference and discharge time. The other important parameters such as energy (E) and power (P) densities have also been evaluated via following equations:

$$E\ (Wh/kg) = 0.5\ CV2/3.6 \quad (2)$$

$$P\ (W/kg) = E \times 3600/t \quad (3)$$

III. RESULTS AND DISCUSSION

III.1 CHARACTERIZATION OF $NIFE_2O_4$, $NIFE_2O_4$/CU-1, AND $NIFE_2O_4$/CU-2

NiFe2O4/Cu-1 and NiFe2O4/Cu-2 were analyzed using FTIR, SEM, TEM, and XRD techniques. The FTIR spectra of NiFe2O4, NiFe2O4/Cu-1, and NiFe2O4/Cu-2 are shown in Figure 2. The important FTIR peaks at 3351, 1763, 1568, 1382, 1062, and 658 cm^{-1} were assigned for $NiFe_2O_4$. The peaks at 3351 and 1568 cm^{-1} were assigned for the O-H bond (stretching and bending). The peak at 1763 cm^{-1} was assigned for C=O (absorbed CO_2). The FTIR peak of 1382 cm^{-1} is due to the C-O (asymmetric) bond. Other peaks at 1060 and 658 cm^{-1} are associated with Ni-Fe, Fe-O, Ni-O, etc. bonds[25], [26], [27]. The important FTIR peaks of $NiFe_2O_4$/Cu-1 were assigned as 3452, 2880, 1527, 1139, and 579 cm^{-1}. These peaks all reveal the presence of O-H, C-H, C-O, Ni-Fe, Fe-Cu, etc. bonds. Similarly, the FTIR peaks of 3425, 2897, 1377, 1086, 879, and 593 cm^{-1} were assigned for $NiFe_2O_4$/Cu-2. These peaks are also revealing the presence of O-H, C-H, C-O, Ni-Fe, Fe-Cu, Cu-O, etc. bonds[25], [26], [28], [29], [30], [31].

XRD patterns of $NiFe_2O_4$, $NiFe_2O_4$/Cu-1, and $NiFe_2O_4$/Cu-2 are depicted in Figure 3. These patterns show that NiFe2O4 is amorphous, while NiFe2O4/Cu-1 and NiFe2O4/Cu-2 are semi-crystalline. The important XRD peaks of $NiFe_2O_4$ were assigned at 2 θ = 30.10 (111), 35.60 (220), 38.70 (222), 43.50 (400), 56.20 (511), 57.40 (511), and 62.70 (440) [32], [33]. The XRD peaks of $NiFe_2O_4$/Cu-1, and $NiFe_2O_4$/Cu-2 were assigned at 2 θ = 30.50 (111), 35.80 (220), 38.70 (222), 43.50 (400), 49.10 (-202), 53.70 (020), 57.50 (511), 61.80 (-113), 62.70 (440), 66.20 (-311), and 68.20 (220), respectively[25], [34], [35], [36], [37], [38]. The morphological features of $NiFe_2O_4$, $NiFe_2O_4$/Cu-1, and $NiFe_2O_4$/Cu-2 were analyzed using SEM technique. Figure 4 depicts the SEM images of $NiFe_2O_4$, $NiFe_2O_4$/Cu-1, and $NiFe_2O_4$/Cu-2. In case of $NiFe_2O_4$, some particles are semi-sphere and some are irregular. After incorporation with Cu, the particles become sphere-shaped. The TEM images (Figure 5) of $NiFe_2O_4$/Cu-2 are also revealing the sphere-shaped particles having average particle size 23.5 nm.

The above-mentioned findings of FTIR and XRD clearly indicate the presence of different main chemical bonds and the nature of the synthesized materials. These techniques provide feasibility of synthetic methods and actual formation of materials. SEM and TEM methods also reveal the actual morphology of $NiFe_2O_4$, $NiFe_2O_4$/Cu-1, and $NiFe_2O_4$/Cu-2.

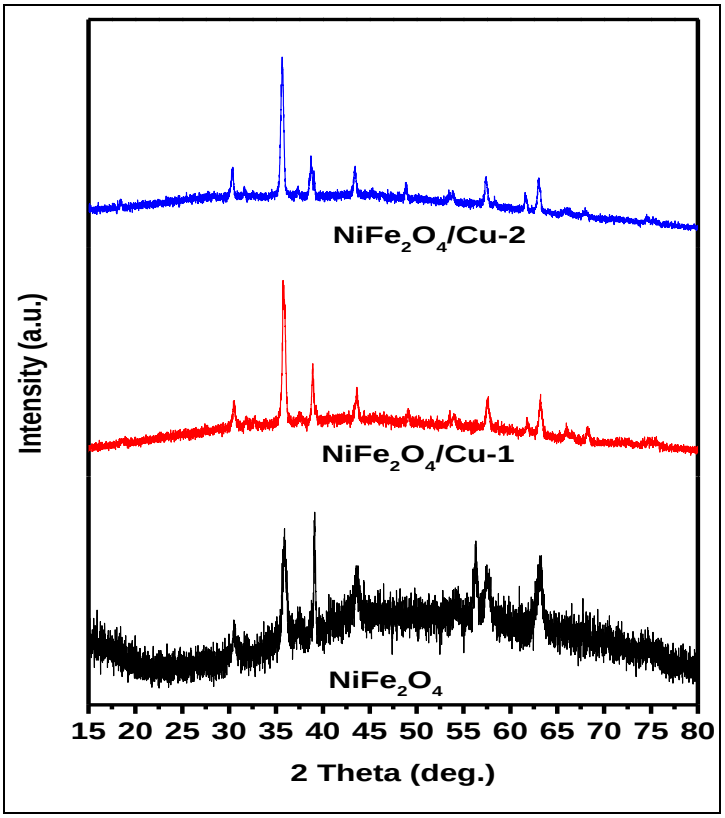

Figure 2: FTIR spectra of NiFe2O4, NiFe2O4/Cu-1, and NiFe2O4/Cu-2.
Source: Authors, (2026).

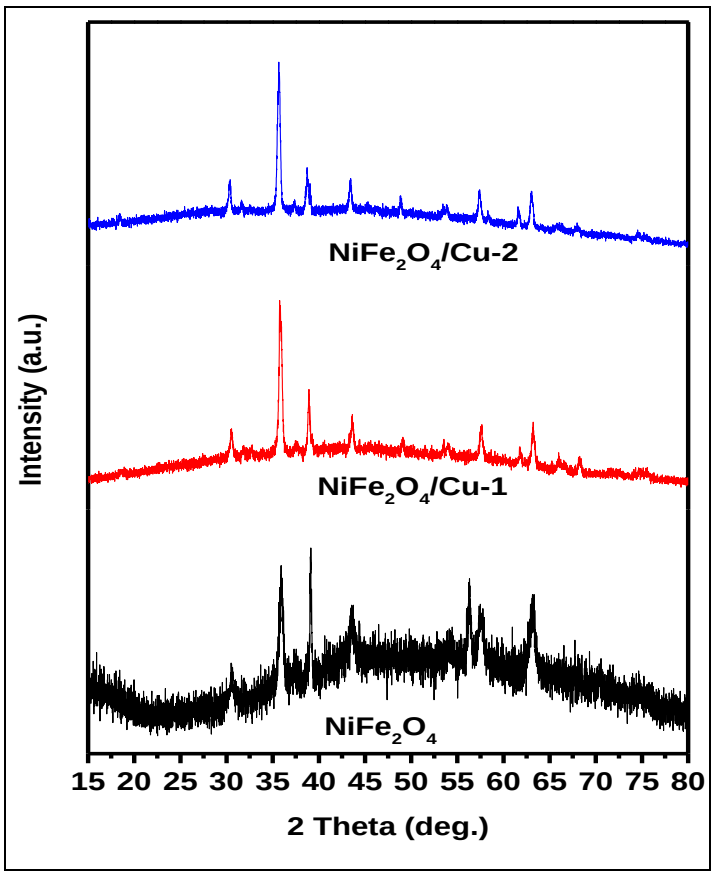

Figure 3: XRD patterns of NiFe2O4, NiFe2O4/Cu-1, and NiFe2O4/Cu-2.
Source: Authors, (2026).

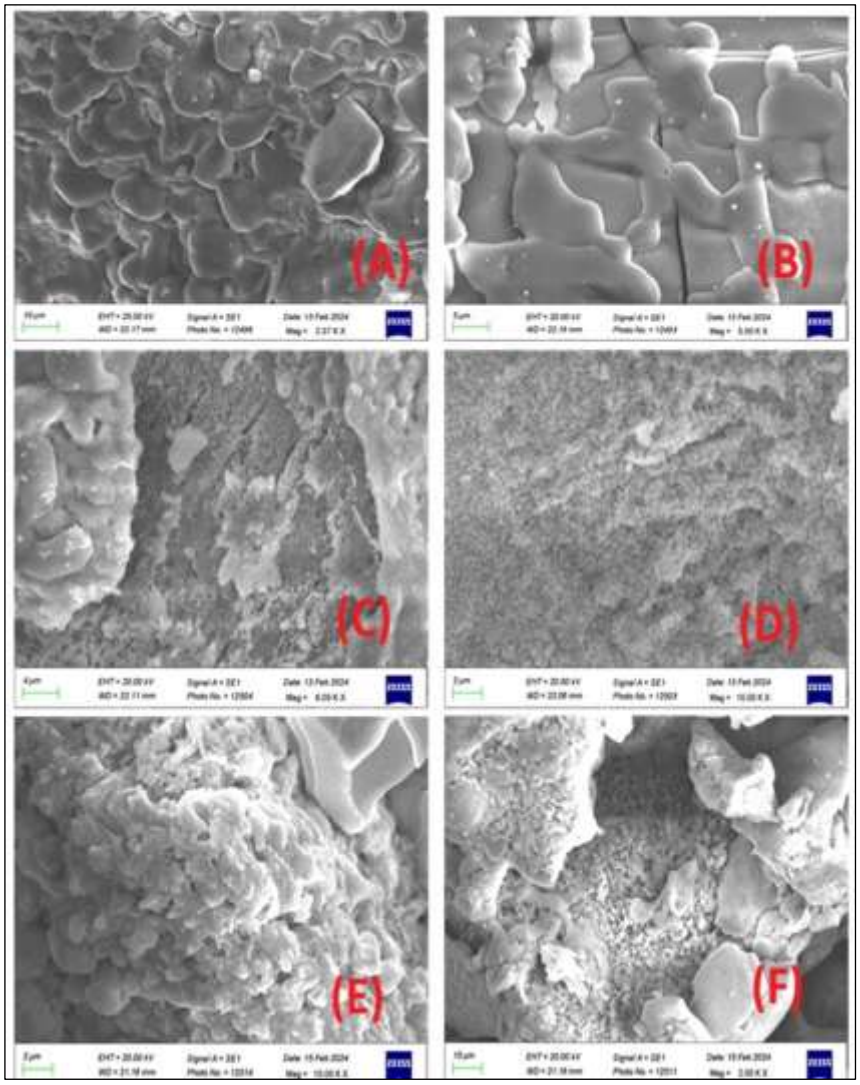

Figure 4: SEM images of NiFe2O4 (A & B), NiFe2O4/Cu-1 (C & D), and NiFe2O4/Cu-2 (E & F).
Source: Authors, (2026).

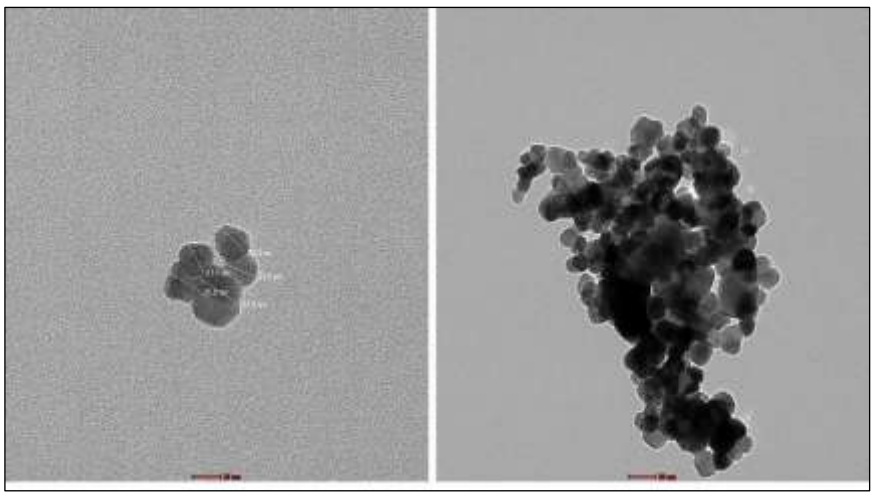

Figure 5: TEM images of NiFe2O4/Cu-2.
Source: Authors, (2026).

III.2 ELECTROCHEMICAL STUDY OF $NIFE_2O_4$, $NIFE_2O_4$/CU-1, AND $NIFE_2O_4$/CU-2

The CV, GCD, and EIS methods were used to analyze the electrochemical behavior of each of these materials. All of these electrochemical parameters are discussed below.

CV

CV is a widely used electrochemical technique for electrode behavior. Static electrode potential is applied at a constant scanning rate throughout CV measurement, and an electron transfer at the active reaction site is used to create a current-potential plot[38], [39][40]. Figure 6 illustrates the CV curves of $NiFe_2O_4$, $NiFe_2O_4$/Cu-1, and $NiFe_2O_4$/Cu-2 under 3 and 2-electrode systems. The CV curves have been obtained at the scan rates of 10, 20, 30, 50, 75, and 100 mV/s. All CV curves have a nearly rectangular shape, which indicates ideal capacitive behavior. Additionally, it shows that an electrical double layer is forming at the electrode-electrolyte interface. The CV curves at various scan rates exhibit a nearly similar rectangular shape, indicating the stability of materials under selected potential windows[41]. The study indicates that as the scan rate increases, the capacitive behavior decreases, indicating that charge dispersion is the primary cause of storage[42]. Similar observation was reported by Al Kiey et al. [43]for the CoFe2O4, CuFe2O4 and Co/CuFe2O4 at the scan rates of 5, 10, 25, 50, 100, and 200 mV/s. Salama et al.[44] also reported similar observations for MgFe2O4 supported on activated carbon at the scan rates of 5, 10, 20, 30, and 50 mV/s, respectively.

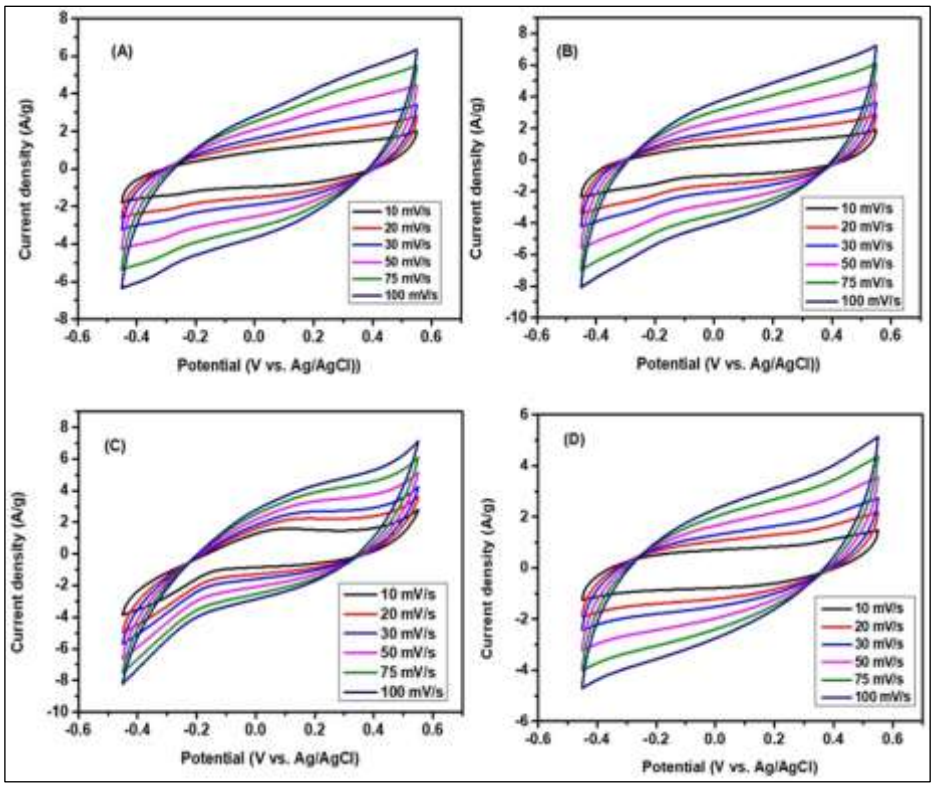

Figure 6: CV curves of (A) NiFe2O4 (under 3-electrode) (B) NiFe2O4/Cu-1 (under 3-electrode) (C) NiFe2O4/Cu-2 (under 3-electrode), and (D) NiFe2O4/Cu-2 (under 2-electrode).
Source: Authors, (2026).

GCD

GCD curves are important parameters for observing the discharge time, retention, and efficiency of electrode materials. The discharge time is directly proportional to the specific capacitance of supercapacitors. The power and energy densities of supercapacitors are also evaluated using GCD curves[42], [45]. The GCD curves of of $NiFe_2O_4$, $NiFe_2O_4$/Cu-1, and $NiFe_2O_4$/Cu-2 under 3 and 2-electrode systems are presented in Figure 7. The GCD curves of $NiFe_2O_4$ are nearly linear and indicating the accumulation of ions at junction of electrode and electrolyte[45]. The small deviation from linearity ($NiFe_2O_4$/Cu-1, and $NiFe_2O_4$/Cu-2) indicates the involvement pseudocapacitive contribution during faradaic reactions[46], [47]. The specific capacitance of $NiFe_2O_4$ was found to be 80, 44, 30.6, 7.6, and 5.2 F/g at the current densities of 2, 4, 6, 8, and 10 A/g. These values increased to 122, 60, 37.8, 18.4, and 18 F/g in the case of $NiFe_2O_4$/Cu-1. At the same current densities, the specific capacitance of $NiFe_2O_4$/Cu-2 was found to be 222, 88, 40.2, 36.8, and 18.6 F/g (Figure 8A). Huynh et al.[48] also reported the similar trend of decrease of specific capacitance of CuFe2O4-based electrode materials at current densities of 0.02, 0.05, 0.1, 0.25, and 0.5 A/g. Kumar et al.[40] also reported the specific capacitance of 295.5, 111.2, 73.3, 71.1, and 33.3F/g for CoFe2O4/Ppy at the current densities of 2, 4, 6, 8, and 10 A/g, respectively.

The specific capacitance of $NiFe_2O_4$/Cu-2 under the 2-electrode system was evaluated to be 42, 24, 18, 16, and 14.5 F/g at the same current densities (Figure 8B). The energy densities of $NiFe_2O_4$/Cu-2 were found to be 5.9, 3.4, 2.5, 2.3, and 2.08 Wh/kg at power densities of 499.9, 1999.8, 3000, 4015.8, and 4992 W/kg, respectively (Figure 8C). The actual efficiency of supercapacitors throughout multiple GCD cycles depends on the cyclic stability of the electrode materials. Several aspects, including redox reversibility, chemical stability, and the structural characteristics of selecetd materials, have a substantial impact on cyclic stability. Materials that are susceptible to irreversible reactions or volume changes frequently deteriorate rapidly. Cu-based materials have high conductivity and reversible redox activity. They provide reliable and effective electrodes when mixed with other substances [15], [16]. $NiFe_2O_4$/Cu-2 was run for 5000 GCD cycles under a 2-electrode system. Retention was found to be 96.7% after the first 500 cycles, which increased to 95.8% after 1500 cycles. After 2500 cycles, retention was achieved to be 94.7%, and it remained 92.8% after 4000 cycles. After 5000 cycles, retention was achieved to be 91.3% (Figure 8D). The comparison of $NiFe_2O_4$/Cu-2 with other electrode materials is shown in table 1.

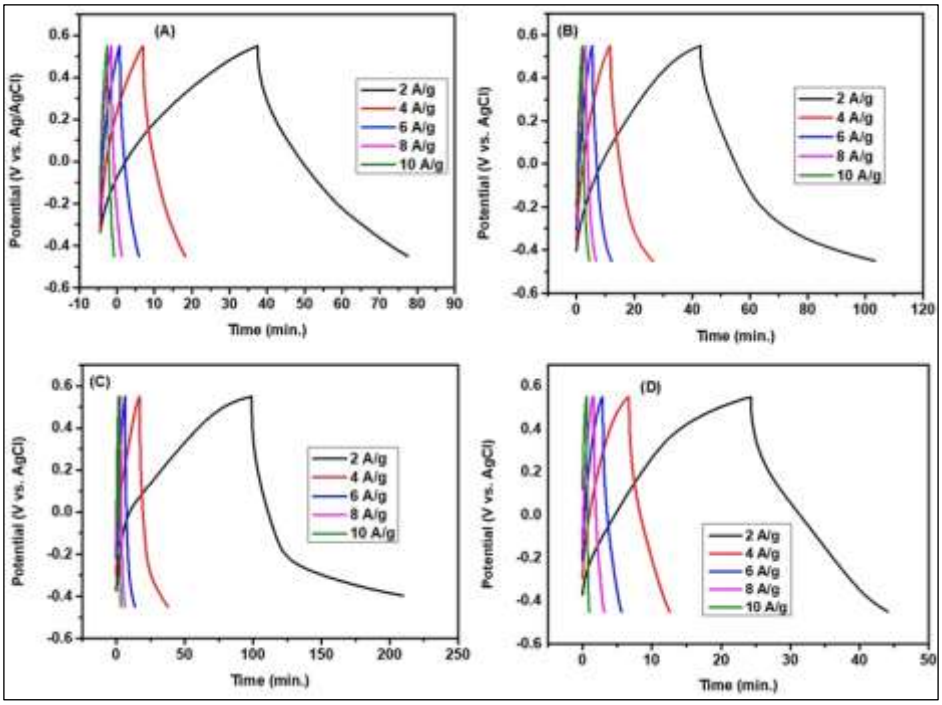

Figure 7: GCD curves of (A) NiFe2O4 (under 3-electrode) (B) NiFe2O4/Cu-1 (under 3-electrode) (C) NiFe2O4/Cu-2 (under 3-electrode), and (D) NiFe2O4/Cu-2 (under 2-electrode).
Source: Authors, (2026).

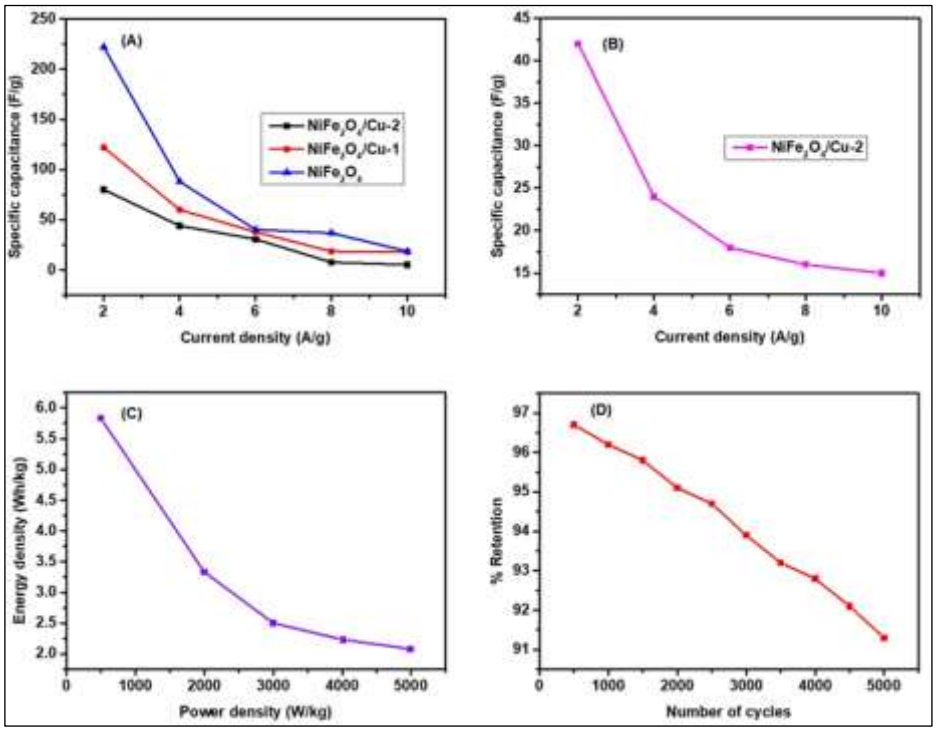

Figure 8: (A) specific capacitance vs current density (under 3-electrode) (B) specific capacitance vs current density (under 2-electrode) (C) energy density vs power density, and (D) cyclization of NiFe2O4/Cu-2 (under 2-electrode).
Source: Authors, (2026).

Table 1: comparison of NiFe2O4/Cu-2 with electrode materials.

Type of electrodes	Maximum specific capacitance	Retention	References
$ZnFe_2O_4$ microspheres	131 F/g	92% after 1000 cycles	[49]
$Ni/ZnFe_2O_4$	504.4 F/g	-	[50]
$CoFe_2O_4$	466 F/g	100% after 10000 cycles	[51]
$CoFe_2O_4$	142 F/g	71.8% after 1000 cycles	[52]
$NiFe_2O_4$	127 F/g	-	[53]
$NiFe_2O_4$/Cu-2	222 F/g	91.3% after 5000 cycles	This study

Source: Authors, (2026).

EIS

Exploring the electrode characteristics of batteries and supercapacitors needs the use of EIS. Furthermore, EIS is utilized in the investigation of corrosion, sensors, and various material properties. [54], [55]. In this study, Nyquist and Bode's curves have been investigated to find out the electrochemical characteristics of $NiFe_2O_4$/Cu-2. A Nyquist plot helps analyze the behavior of a supercapacitor by visualizing its complex impedance at various frequencies. The Nyquist curve of $NiFe_2O_4$/Cu-2 is shown in Figure 9 A. This curve shows the ideal capacitive behavior of selected electrode material[56]. This curve indicates the unique charge-transfer process between the electrode and electrolyte[57]. Bode's curves (Figure 9B) examine the features of impedance in electrochemical systems and demonstrate that resistive components allow impedance to become constant at high frequencies. Bulk electrolyte, electrode features, and interface resistances also contribute to this resistance. Understanding these elements is essential for enhancing device reliability and material design[39], [57], [58].

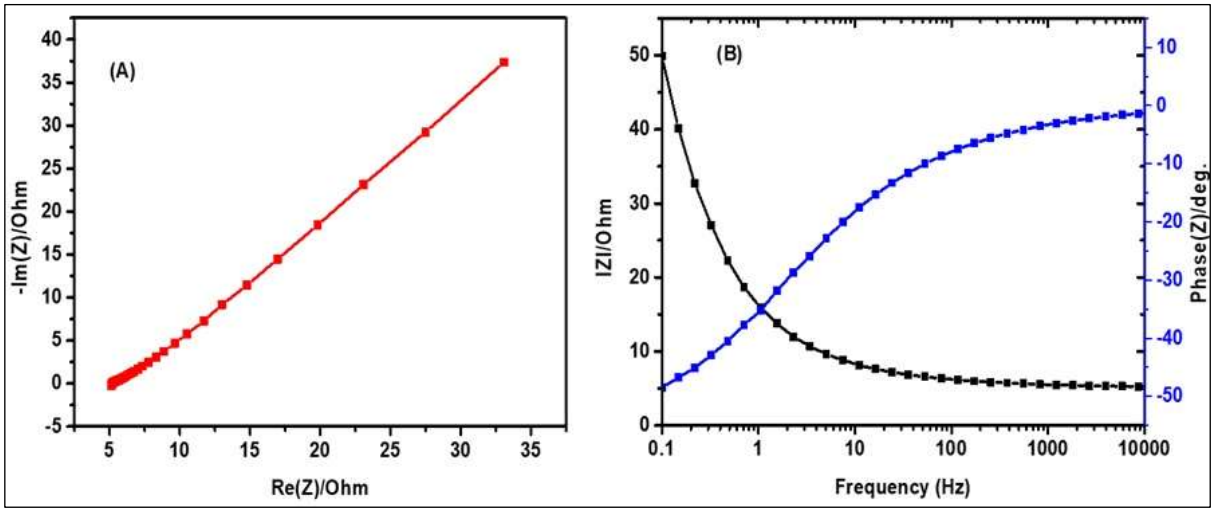

Figure 9: (A) Nyquist curve, and (B) Bode's curve of $NiFe_2O_4$/Cu-2.
Source: Authors, (2026).

IV. CONCLUSION

The primary objectives of energy storage in the future are to increase sustainability, capacity, and efficiency. Supercapacitors provide fast charge/discharge, stability, and a high-power density, making them promising energy storage devices. Future advancements in electrode materials for supercapacitors are expected as researchers continue to explore and develop more sophisticated and high-performance materials. Ferrite-based materials have a lot of potential as supercapacitor electrode materials due to their inexpensiveness, environmental friendliness, and multiple oxidation states. With an energy density of 5.9 Wh/kg, a specific capacitance of 222 F/g at 2 A/g, and 91.3% retention after 5000 cycles under a 2-electrode system, the developed $NiFe_2O_4$/Cu-2 showed enhanced electrochemical capabilities. The important characteristics of NiFe2O4/Cu-2 have also been investigated using different characterization techniques such as FTIR, XRD, SEM, and TEM, respectively. The specific capacitance under the 2-electrode system was found to be 42 F/g, and the NiFe2O4/Cu-2 was also found to be a promising material for the device system.

V. ACKNOWLEDGEMENT

We are thankful to Department of Chemistry, Graphic Era (Deemed to be University), and Division of Research and Innovation, Uttaranchal University, Dehradun (India) for the support and encouragement.

VI. AUTHORSHIP CONTRIBUTION STATEMENT

Conceptualization: Khundrakpam Somen Singh, Naveen Chandra Joshi, B.S.Rawat.
Methodology: Khundrakpam Somen Singh.
Investigation: Khundrakpam Somen Singh, Naveen Chandra Joshi**.**
Discussion of results: Khundrakpam Somen Singh, Naveen Chandra Joshi, B.S.Rawat.
Writing – Original Draft: Naveen Chandra Joshi.
Writing – Review and Editing: B.S.Rawat.
Resources: Khundrakpam Somen Singh, Naveen Chandra Joshi, B.S.Rawat.
Supervision: Khundrakpam Somen Singh, Naveen Chandra Joshi, B.S.Rawat.
Approval of the final text: Khundrakpam Somen Singh, Naveen Chandra Joshi, B.S.Rawat.

VII. REFERENCES

[1] G. G. Njema, R. B. O. Ouma, and J. K. Kibet, "A Review on the Recent Advances in Battery Development and Energy Storage Technologies," Journal of Renewable Energy, vol. 2024, pp. 1–35, May 2024, doi: 10.1155/2024/2329261.

[2] X.-P. Zhang, "Development of European Energy Internet and the role of Energy Union," in The Energy Internet, Elsevier, 2019, pp. 347–367. doi: 10.1016/B978-0-08-102207-8.00015-1.

[3] K. Chen and D. Xue, “Searching for electrode materials with high electrochemical reactivity,” Journal of Materiomics, vol. 1, no. 3, pp. 170–187, Sep. 2015, doi: 10.1016/j.jmat.2015.07.001.

[4] S. G. Sayyed, A. V. Shaikh, U. P. Shinde, P. Hiremath, and N. Naik, “Copper oxide-based high-performance symmetric flexible supercapacitor: potentiodynamic deposition,” Journal of Materials Science: Materials in Electronics, vol. 34, no. 17, p. 1361, Jun. 2023, doi: 10.1007/s10854-023-10738-7.

[5] M. Mustaqeem et al., “Rational design of Cu based composite electrode materials for high-performance supercapacitors – A review,” J Energy Storage, vol. 51, p. 104330, Jul. 2022, doi: 10.1016/j.est.2022.104330.

[6] M. Z. Iqbal, S. Zakar, and S. S. Haider, “Role of aqueous electrolytes on the performance of electrochemical energy storage device,” Journal of Electroanalytical Chemistry, vol. 858, p. 113793, Feb. 2020, doi: 10.1016/j.jelechem.2019.113793.

[7] A. Mendhe and H. S. Panda, “A review on electrolytes for supercapacitor device,” Discov Mater, vol. 3, no. 1, p. 29, Oct. 2023, doi: 10.1007/s43939-023-00065-3.

[8] Reenu, Sonia, L. Phor, A. Kumar, and S. Chahal, “Electrode materials for supercapacitors: A comprehensive review of advancements and performance,” J Energy Storage, vol. 84, p. 110698, Apr. 2024, doi: 10.1016/j.est.2024.110698.

[9] N. Maji and H. S. Dosanjh, “Ferrite Nanoparticles as Catalysts in Organic Reactions: A Mini Review,” Magnetochemistry, vol. 9, no. 6, p. 156, Jun. 2023, doi: 10.3390/magnetochemistry9060156.

[10] S. J. Salih and W. M. Mahmood, “Review on magnetic spinel ferrite (MFe2O4) nanoparticles: From synthesis to application,” Heliyon, vol. 9, no. 6, p. e16601, Jun. 2023, doi: 10.1016/j.heliyon.2023.e16601.

[11] N. Kumari, S. Kour, G. Singh, and R. K. Sharma, “A brief review on synthesis, properties and applications of ferrites,” 2020, p. 020164. doi: 10.1063/5.0001323.

[12] J. Patra and V. K. Verma, “Nickel ferrite: Advances in the synthesis methods, properties and its applications,” Nano-Structures & Nano-Objects, vol. 42, p. 101458, May 2025, doi: 10.1016/j.nanoso.2025.101458.

[13] R. S. Rajenimbalkar, V. J. Deshmukh, K. K. Patankar, and S. B. Somvanshi, “Effect of multivalent ion doping on magnetic, electrical, and dielectric properties of nickel ferrite nanoparticles,” Sci Rep, vol. 14, no. 1, p. 29547, Nov. 2024, doi: 10.1038/s41598-024-81222-3.

[14] M. S. Rathod, A. C. Mehere, P. B. Kadam, S. V. Gaikwad, S. K. Jagadale, and S. M. Rathod, “Boosting nickel nanoferrite’s specific capacitance with Azadirachta Indica for advanced supercapacitors,” Inorg Chem Commun, vol. 170, p. 113265, Dec. 2024, doi: 10.1016/j.inoche.2024.113265.

[15] D. Majumdar and S. Ghosh, “Recent advancements of copper oxide based nanomaterials for supercapacitor applications,” J Energy Storage, vol. 34, p. 101995, Feb. 2021, doi: 10.1016/j.est.2020.101995.

[16] K. Pandey, P. Yadav, and I. Mukhopadhyay, “Elucidating the effect of copper as a redox additive and dopant on the performance of a PANI based supercapacitor,” Physical Chemistry Chemical Physics, vol. 17, no. 2, pp. 878–887, 2015, doi: 10.1039/C4CP04321A.

[17] W. T. Infancy et al., “Nickel-infused cobalt ferrite/MXene nanocomposites: Structural insights and electrochemical properties for high performance supercapacitors,” Inorg Chem Commun, vol. 181, p. 115156, Nov. 2025, doi: 10.1016/j.inoche.2025.115156.

[18] S. Mandal and A. K. Dasmahapatra, “Hierarchical polyaniline/copper cobalt ferrite nanocomposites for high performance supercapacitor electrode,” J Energy Storage, vol. 74, p. 109402, Dec. 2023, doi: 10.1016/j.est.2023.109402.

[19] V. Vignesh, K. Subramani, M. Sathish, and R. Navamathavan, “Electrochemical investigation of manganese ferrites prepared via a facile synthesis route for supercapacitor applications,” Colloids Surf A Physicochem Eng Asp, vol. 538, pp. 668–677, Feb. 2018, doi: 10.1016/j.colsurfa.2017.11.045.

[20] K.-Y. Shih and H.-Y. Tseng, “One-Step Microwave-Assisted Synthesis of MnFe 2 O 4 /rGO Nanocomposites and Their Electrochemical Properties in Supercapacitors,” ACS Omega, vol. 10, no. 5, pp. 4473–4485, Feb. 2025, doi: 10.1021/acsomega.4c07810.

[21] V. K. Undavalli, C. Ling, and B. Khandelwal, “Impact of alternative fuels and properties on elastomer compatibility,” in Aviation Fuels, Elsevier, 2021, pp. 113–132. doi: 10.1016/B978-0-12-818314-4.00001-7.

[22] N. Raval, R. Maheshwari, D. Kalyane, S. R. Youngren-Ortiz, M. B. Chougule, and R. K. Tekade, “Importance of Physicochemical Characterization of Nanoparticles in Pharmaceutical Product Development,” in Basic Fundamentals of Drug Delivery, Elsevier, 2019, pp. 369–400. doi: 10.1016/B978-0-12-817909-3.00010-8.

[23] Y. R. Herrero, K. L. Camas, and A. Ullah, “Characterization of biobased materials,” in Advanced Applications of Biobased Materials, Elsevier, 2023, pp. 111–143. doi: 10.1016/B978-0-323-91677-6.00005-2.

[24] A. Mondal, P. Debnath, and N. K. Mondal, “Nanoparticles: A new tool for control of mosquito larvae,” in Intelligent Environmental Data Monitoring for Pollution Management, Elsevier, 2021, pp. 49–70. doi: 10.1016/B978-0-12-819671-7.00003-8.

[25] T. M. Naidu and P. V. L. Narayana, “Synthesis and Characterization of Fe-TiO2 and NiFe2O4 Nanoparticles and Its Thermal Properties,” Journal of Nanoscience and Technology, vol. 5, no. 4, pp. 769–772, Jun. 2019, doi: 10.30799/jnst.247.19050407.

[26] M. A. Fathy, A. H. Kamel, and S. S. M. Hassan, “Novel magnetic nickel ferrite nanoparticles modified with poly(aniline- co-o -toluidine) for the removal of hazardous 2,4-dichlorophenol pollutant from aqueous solutions,” RSC Adv, vol. 12, no. 12, pp. 7433–7445, 2022, doi: 10.1039/D2RA00034B.

[27] M. Shafiey Dehaj and M. Zamani Mohiabadi, “Experimental study of water-based CuO nanofluid flow in heat pipe solar collector,” J Therm Anal Calorim, vol. 137, no. 6, pp. 2061–2072, Sep. 2019, doi: 10.1007/s10973-019-08046-6.

[28] K. S. A. Ali, V. Mohanavel, C. Gnanavel, V. Vijayan, and N. Senthilkumar, “Structural and optical behavior of SnS2/NiFe2O4 NCs prepared via novel two-step synthesis approach for MB and RhB dye degradation under sun light irradiation,” Research on Chemical Intermediates, vol. 47, no. 5, pp. 1941–1954, May 2021, doi: 10.1007/s11164-021-04401-1.

[29] M. Shafiey Dehaj and M. Zamani Mohiabadi, “Experimental study of water-based CuO nanofluid flow in heat pipe solar collector,” J Therm Anal Calorim, vol. 137, no. 6, pp. 2061–2072, Sep. 2019, doi: 10.1007/s10973-019-08046-6.

[30] A. Varughese, R. Kaur, and P. Singh, “Green Synthesis and Characterization of Copper Oxide Nanoparticles Using Psidium guajava Leaf Extract,” IOP Conf Ser Mater Sci Eng, vol. 961, no. 1, p. 012011, Nov. 2020, doi: 10.1088/1757-899X/961/1/012011.

[31] M. A. T. G. N. C. A. B. Bodade, “Bioelectrode based chitosan-nano copper oxide for application to lipase biosensor,” Journal of Applied Pharmaceutical Research, vol. 5, pp. 30–39, 2017.

[32] S. Sobhanardakani, R. Zandipak, H. Khoshsafar, and R. Zandipak, “Removal of cationic dyes from aqueous solutions using NiFe 2 O 4 nanoparticles,” Journal of Water Supply: Research and Technology - Aqua, p. jws2015046, Nov. 2015, doi: 10.2166/aqua.2015.046.

[33] D. Zhu, L. Wang, W. Yu, and H. Xie, “Intriguingly high thermal conductivity increment for CuO nanowires contained nanofluids with low viscosity,” Sci Rep, vol. 8, no. 1, p. 5282, Mar. 2018, doi: 10.1038/s41598-018-23174-z.

[34] S. Sobhanardakani, R. Zandipak, H. Khoshsafar, and R. Zandipak, “Removal of cationic dyes from aqueous solutions using NiFe 2 O 4 nanoparticles,” Journal of Water Supply: Research and Technology - Aqua, p. jws2015046, Nov. 2015, doi: 10.2166/aqua.2015.046.

[35] V. Manikandan et al., “Efficient humidity-sensitive electrical response of annealed lithium substituted nickel ferrite (Li–NiFe2O4) nanoparticles under ideal, real and corrosive environments,” Journal of Materials Science: Materials in Electronics, vol. 29, no. 21, pp. 18660–18667, Nov. 2018, doi: 10.1007/s10854-018-9987-y.
[36] D. Zhu, L. Wang, W. Yu, and H. Xie, “Intriguingly high thermal conductivity increment for CuO nanowires contained nanofluids with low viscosity,” Sci Rep, vol. 8, no. 1, p. 5282, Mar. 2018, doi: 10.1038/s41598-018-23174-z.

[37] S. Sagadevan, K. Pal, and Z. Z. Chowdhury, “Fabrication of CuO nanoparticles for structural, optical and dielectric analysis using chemical precipitation method,” Journal of Materials Science: Materials in Electronics, vol. 28, no.
17, pp. 12591–12597, Sep. 2017, doi: 10.1007/s10854-017-7083-3.

[38] P. Batista Deroco, J. de F. Giarola, D. Wachholz Júnior, G. Arantes Lorga, and L. Tatsuo Kubota, “Paper-based electrochemical sensing devices,” 2020, pp. 91–137. doi: 10.1016/bs.coac.2019.11.001.

[39] N. Bhuvanendran, S. Ravichandran, Q. Xu, T. Maiyalagan, and H. Su, “A quick guide to the assessment of key electrochemical performance indicators for the oxygen reduction reaction: A comprehensive review,” Int J Hydrogen Energy, vol. 47, no. 11, pp. 7113–7138, Feb. 2022, doi: 10.1016/j.ijhydene.2021.12.072.

[40] S. Kumar, N. Chandra Joshi, B. S. Rawat, and P. Gururani, “Synthesis and electrochemical potential of CoFe2O4/Ppy-based material,” Inorg Chem Commun, vol. 167, p. 112692, Sep. 2024, doi: 10.1016/j.inoche.2024.112692.

[41] R. Tholkappiyan, A. N. Naveen, K. Vishista, and F. Hamed, “Investigation on the electrochemical performance of hausmannite Mn 3 O 4 nanoparticles by ultrasonic irradiation assisted co-precipitation method for supercapacitor electrodes,” Journal of Taibah University for Science, vol. 12, no. 5, pp. 669–677, Sep. 2018, doi: 10.1080/16583655.2018.1497440.

[42] Z. Ren, J. Li, Y. Ren, S. Wang, Y. Qiu, and J. Yu, “Large-scale synthesis of hybrid metal oxides through metal redox mechanism for high-performance pseudocapacitors,” Sci Rep, vol. 6, no. 1, p. 20021, Jan. 2016, doi:
10.1038/srep20021.

[43] S. A. Al Kiey, R. Ramadan, and M. M. El-Masry, “Synthesis and characterization of mixed ternary transition metal ferrite nanoparticles comprising cobalt, copper and binary cobalt–copper for high-performance supercapacitor applications,” Applied Physics A, vol. 128, no. 6, p. 473, Jun. 2022, doi: 10.1007/s00339-022-05590-1.

[44] Reda. S. Salama, M. S. Gouda, M. F. A. Aboud, F. T. Alshorifi, A. A. El-Hallag, and A. K. Badawi, “Synthesis and characterization of magnesium ferrite-activated carbon composites derived from orange peels for enhanced supercapacitor performance,” Sci Rep, vol. 14, no. 1, p. 8223, Apr. 2024, doi: 10.1038/s41598-024-54942-9.

[45] B. Raut et al., “Battery-Type Transition Metal Oxides in Hybrid Supercapacitors: Synthesis and Applications,” Batteries, vol. 11, no. 2, p. 60, Feb. 2025, doi: 10.3390/batteries11020060.

[46] S. Sharma and P. Chand, “Supercapacitor and electrochemical techniques: A brief review,” Results Chem, vol. 5, p. 100885, Jan. 2023, doi: 10.1016/j.rechem.2023.100885.

[47] Y. Zhang, X. Li, Z. Li, and F. Yang, “Evaluation of electrochemical performance of supercapacitors from equivalent circuits through cyclic voltammetry and galvanostatic charge/discharge,” J Energy Storage, vol. 86, p. 111122, May 2024, doi: 10.1016/j.est.2024.111122.

[48] K. Huynh, B. Maddipudi, and R. Shende, “Hybrid Mesoporous Carbon/Copper Ferrite Electrode for Asymmetric Supercapacitors,” Nanomaterials, vol. 13, no. 16, p. 2365, Aug. 2023, doi: 10.3390/nano13162365.

[49] M. Zhu, X. Zhang, Y. Zhou, C. Zhuo, J. Huang, and S. Li, “Facile solvothermal synthesis of porous ZnFe 2 O 4 microspheres for capacitive pseudocapacitors,” RSC Adv, vol. 5, no. 49, pp. 39270–39277, 2015, doi: 10.1039/C5RA00447K.

[50] B. Nawaz, G. Ali, M. O. Ullah, S. Rehman, and F. Abbas, “Investigation of the Electrochemical Properties of Ni0.5Zn0.5Fe2O4 as Binder-Based and Binder-Free Electrodes of Supercapacitors,” Energies (Basel), vol. 14, no. 11, p. 3297, Jun. 2021, doi: 10.3390/en14113297.

[51] M. Malarvizhi et al., “Design and fabrication of cobalt and nickel ferrites based flexible electrodes for high-performance energy storage applications,” Inorg Chem Commun, vol. 123, p. 108344, Jan. 2021, doi:
10.1016/j.inoche.2020.108344.

[52] L. Lv, Q. Xu, R. Ding, L. Qi, and H. Wang, “Chemical synthesis of mesoporous CoFe2O4 nanoparticles as promising bifunctional electrode materials for supercapacitors,” Mater Lett, vol. 111, pp. 35–38, Nov. 2013, doi: 10.1016/j.matlet.2013.08.055.

[53] P. Sen and A. De, “Electrochemical performances of poly(3,4-ethylenedioxythiophene)–NiFe2O4 nanocomposite as electrode for supercapacitor,” Electrochim Acta, vol. 55, no. 16, pp. 4677–4684, Jun. 2010, doi: 10.1016/j.electacta.2010.03.077.

[54] S. Wang, J. Zhang, O. Gharbi, V. Vivier, M. Gao, and M. E. Orazem, “Electrochemical impedance spectroscopy,” Nature Reviews Methods Primers, vol. 1, no. 1, p. 41, Jun. 2021, doi: 10.1038/s43586-021-00039-w.

[55] I. K. Durga, K. V. G. Raghavendra, N. B. Kundakarla, S. Alapati, J.-W. Ahn, and S. Srinivasa Rao, "Facile Synthesis of Coral Reef-Like ZnO/CoS2 Nanostructure on Nickel Foam as an Advanced Electrode Material for High-Performance Supercapacitors," Energies (Basel), vol. 14, no. 16, p. 4925, Aug. 2021, doi: 10.3390/en14164925.

[56] H. S. Magar, R. Y. A. Hassan, and A. Mulchandani, "Electrochemical Impedance Spectroscopy (EIS): Principles, Construction, and Biosensing Applications," Sensors, vol. 21, no. 19, p. 6578, Oct. 2021, doi: 10.3390/s21196578.

[57] B. A. Mei, O. Munteshari, J. Lau, B. Dunn, and L. Pilon, "Physical Interpretations of Nyquist Plots for EDLC Electrodes and Devices," Journal of Physical Chemistry C, vol. 122, no. 1, 2018, doi: 10.1021/acs.jpcc.7b10582.

[58] N. C. Joshi, P. Gururani, and N. Kumar, "Electrochemical performance of SnO2 after blending with Cu," Ionics (Kiel), vol. 30, no. 10, pp. 6531–6547, Oct. 2024, doi: 10.1007/s11581-024-05742-8.